 doi:10.20944/preprints201905.0171.v1

Research Article

Differential role of TGF-β in extracellular matrix regulation during *Trypanosoma cruzi* - host cell interaction

Tatiana Araújo Silva, Luis Felipe de Carvalho Ferreira, Mirian Claudia de Souza Pereira and Claudia Magalhães Calvet*.

Cellular Ultrastructure Laboratory, Oswaldo Cruz Institute, FIOCRUZ, Rio de Janeiro, RJ, 21040-360, Brazil

*Corresponding author: Dr Claudia M. Calvet, Laboratório de Ultraestrutura Celular, Instituto Oswaldo Cruz, FIOCRUZ, Av. Brasil 4365, Manguinhos, 21040-362 Rio de Janeiro, RJ, Brazil, e-mail: cmcalvet@ioc.fiocruz.br; claudiacalvet@gmail.com

 doi:10.20944/preprints201905.0171.v1

Abstract

Transforming growth factor beta (TGF-β) is a determinant for inflammation and fibrosis in cardiac and skeletal muscle in Chagas disease. To determine its regulatory mechanisms, we investigated the response of *T. cruzi*-infected cardiomyocytes (CM), cardiac fibroblasts (CF) and L6E9 skeletal myoblasts to TGF-β. Cultures of CM, CF and L6E9 were infected with *T. cruzi* (Y strain) and treated with TGF-β (1-10 ng/ml, 1h or 48h). Fibronectin (FN) distribution was analyzed by immunofluorescence and Western blot (WB). Phosphorylated SMAD2 (PS2), phospho-p38 (p-p38), and phospho-c-Jun (p-c-Jun) signaling were evaluated by WB. CF and L6E9 showed an increase in FN from 1 ng/ml of TGF-β, while CM displayed FN modulation only after 10 ng/ml treatment. CF and L6E9 showed higher PS2 levels than CM, while p38 is less stimulated in CF than CM and L6E9. After *T. cruzi* infection, localized FN disorganization was observed in infected CF and L6E9. *T. cruzi* induced an increase in FN in CF cultures, mainly in uninfected cells. Infected CF cultures treated with TGF-β showed a reduction in PS2 and an increase in p-p38 and p-c-Jun levels. Our data suggest that p38 and c-Jun pathways may be participating in the fibrosis regulatory process mediated by TGF-β after *T. cruzi* infection.

Keywords: *Trypanosoma cruzi*; TGF-β; Heart fibrosis; Extracellular matrix; Signaling pathways; SMAD2; p-38 MAPK; c-Jun.

 doi:10.20944/preprints201905.0171.v1

1. Introduction

Chagas disease (CD), caused by the flagellated protozoan *Trypanosoma cruzi* [1], currently affects 6-8 million people worldwide [2]. The disease scenario has shifted to a global threat due to migration of infected individuals to non-endemic areas [3,4]. CD presents in acute and chronic clinical forms. . While the former is typically inapparent or presents only mild manifestations and commonly ignored due to non-specific signs, the latter, although asymptomatic in approximately 70% of cases, may progress to severe damage. Muscular pain and weakness are also frequent symptoms in chagasic patients [5]. Chronic Chagas cardiomyopathy (CCC), estimated to be present in 20-30% of infected individuals [6,7], is the most severe manifestation in CD, with a high morbidity and mortality, has significant economic and social impacts in Latin America [8].

In CD, cardiomyopathy is characterized by an intense myocarditis, related to the presence of inflammatory cells reacting to the parasite, resulting in cardiac tissue damage and fibrosis [9]. Skeletal muscle tissue also presents parasitism and inflammation in myofibers [5,10]. Cardiac fibroblasts are the main actors in fibrotic processes acting on the remodeling of extracellular matrix (ECM) in the myocardium [11]. External stimuli, including chemokines and cytokines, regulate fibroblast proliferation and ECM synthesis and secretion [12].

Transforming growth factor β (TGF-β), a cytokine involved in various biological and physiological processes [13], has been highlighted as a regulator of the fibrotic process in the pathogenesis of Chagas disease [14,15]. The signaling pathway of the TGF-β family occurs through three receptors, type I (TGFβI), II (TGFβII) and III (TGFβIII). Type III receptors, also called betaglycans or endoglycans, act as co-receptors, presenting the cytokine to its specific receptors. The binding of active TGF-β to the TGFβII propagates the signal via downstream effectors with the phosphorylation of proteins from the TGF-β classical (canonical) signaling pathway and SMAD proteins (SMADS 1-7) [16]. In addition to the classical signaling pathway, TGF-β also modulates non-canonical signaling pathways, such as p38 mitogen-activated protein kinase (p38MAPK), extracellular signal regulated kinase (ERK), c-Jun N-terminal kinase (JNK), Nuclear factor-kB (NF-kB) and small GTPases [17,18]. JNK and p38MAPK are the alternative routes of TGF-β signaling best characterized. The JNK and p38 MAPK pathways are activated by MAP kinase (MKKs) MKK4 and MKK 3/6, respectively. TGF-β also triggers the activation of TGF-β1-associated kinases (TAK1) through the catalytic activation of factor-associated tumor necrosis factor receptor 6 (TRAF6), crucial processes for the activation of JNK and p38 MAPK [19].

TGF-β plays an important role in *T. cruzi* biology. This cytokine is involved in the host cell invasion process, since *T. cruzi* requires functional TGF-β receptors and activation of its classical signaling pathway to invade the host cell [20–22]. Also, amastigote forms capture TGF-β from the host cell, using it for differentiation into the trypomastigote form, which allows the completion of the

 doi:10.20944/preprints201905.0171.v1

parasite intracellular cycle [23]. Experimental evidence also shows that the parasite induces the synthesis of TGF-β in cardiomyocytes and cardiac fibroblasts [24], which may influence the survival of the parasite. Trypomastigote and amastigote forms are able to directly activate latent TGF-β through its main cysteine peptidase (CP), cruzipain, [25,26], which may contribute to the invasion process and the genesis of Chagas disease.

In addition, the host immune response is controlled by TGF-β during *T. cruzi* infection [27–29]. Elevated TGF-β levels were associated with intense myocardial fibrosis detected in *T. cruzi*-infected α2-macrobulin knockout mice [28] and in patients with CCC [30]. TGF-β receptor expression was increased in *T. cruzi*-infected mouse hearts, in association with increased collagen I and fibronectin expression in myocardium [31]. Recent reports describe that TGF-β inhibitors reduce infection and prevent cardiac damage and fibrosis during experimental *T. cruzi-* infection [32–36]. Taken together, these evidences show a key role of TGF-β in *T. cruzi* infection and in Chagas disease cardiomyopathy.

Besides the known enhancement of ECM during fibrosis process in vivo, our group demonstrated that cardiomyocytes highly infected with *T. cruzi* (72 and 96 h of infection) *in vitro* present low fibronectin expression, while adjacent non-infected cells show an intense network of extracellular matrix component similar to the control [37], even after treatment with TGF-β [34]. Although TGF-β treatment is able to trigger the increase of ECM expression in uninfected cardiomyocytes, the effect is dose dependent, being observed only after the treatment with high concentrations of TGF-β (> 10 ng/ml) [34].

Given that cardiac fibroblasts, the main cell type responsible for ECM synthesis in the myocardium, are the effector cells in the cardiac fibrosis process, [38], and that cell lines originated from skeletal muscle (skeletal myoblasts L6E9) respond to TGF-β in picomolar concentrations [39], we evaluated the expression of extracellular matrix components in uninfected and *T. cruzi*-infected cardiac fibroblasts and skeletal muscle cells (L6E9) after treatment with different concentrations of TGF-β, and analyzed the underlying signaling mechanisms of these processes.

2. Results

2.1. Modulation of fibronectin spatial distribution in different cell types after TGF-β stimulation.

In an attempt to understand the mechanisms underlying cardiac fibrosis evidenced in the pathogenesis of Chagas disease, we evaluated the modulation of extracellular matrix components in cardiomyocytes (CM), cardiac fibroblasts (CFs) and L6E9 skeletal myoblasts stimulated with TGF-β, an important mediator of the fibrosis process. First, the distribution of fibronectin (FN) fibrils in the ECM of these cell types was analyzed in response to stimulation of TGF-β (1-10 ng/ml) for 48 h by indirect immunofluorescence. Purified CF cultures were achieved

 doi:10.20944/preprints201905.0171.v1

after the 5th culture passage of cardiomyocyte (CM) cultures as determined by the absence of Western blot reactivity for desmin, intermediate filament proteins specifically expressed in CM (*supplemental data S1*). Confocal microscopy revealed the arrangement of FN fibrils on the CM surface, evidencing a thickening at the FN network dependent on cytokine stimulus concentration (Fig. 1). The profile of FN distribution in the ECM remained similar to the untreated cells (Fig. 1A) even after stimulation with TGF-β at 1 ng/ml (Fig. 1B). However, CMs stimulated with 10 ng/ml of TGF-β (Fig. 1C) displayed an increase in the thickness of FN fibrils in the ECM, as previously reported (Calvet et al., 2009). In contrast, an increase in FN fibrils was revealed at the surface of L6E9 skeletal myoblasts (Fig. 1E) and CFs (Fig. 1H) after stimulation with 1 ng/ml of TGF-β, a dose 10 times lower than that required to stimulate CMs. The enhancement of FN deposit occurred in a dose-dependent manner showing thicker FN fibrillar network after treatment of L6E9 skeletal myoblasts (Fig. 1F) and CF (Fig. 1I) with 10 ng/ml of the cytokine.

Preprints (www.preprints.org) | NOT PEER-REVIEWED | Posted: 14 May 2019 doi:10.20944/preprints201905.0171.v1

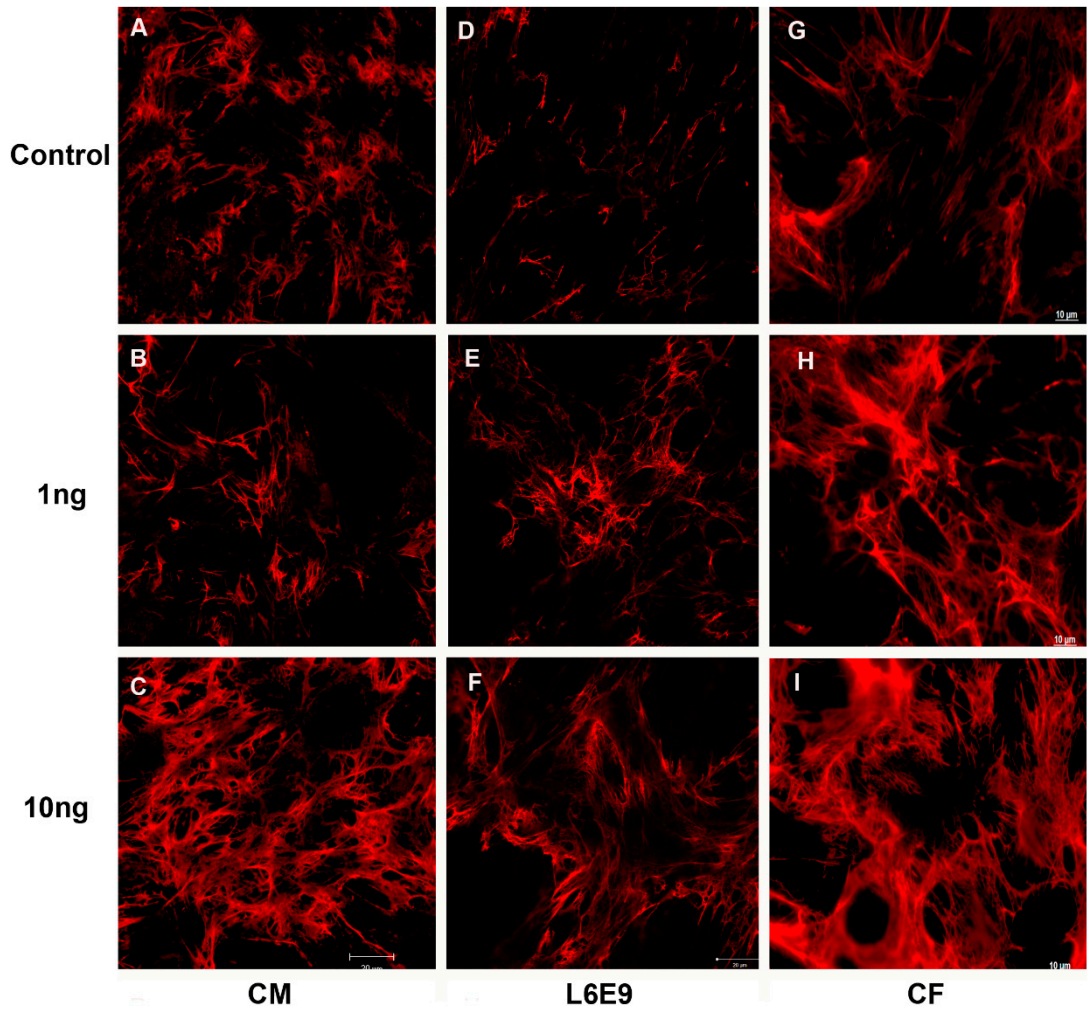

Figure 1 – TGF-β differentially modulates FN in cardiomyocytes, skeletal myoblasts L6E9 and cardiac fibroblasts uninfected. (A) Normal cardiomyocytes show FN fibrils on surface. The addition of 1 ng/ml (B) or 10 ng/ml (C) TGF-β does not alter the FN expression in normal cardiomyocytes. Only 10 ng/ml of TGF-β induces the increase of FN expression (D). In contrast, L6E9 skeletal myoblasts (E) and cardiac fibroblasts (H) present the FN matrix stimulation after treatment with 1 ng/ml TGF-β when compared to untreated cultures (D and G). The FN increase is still detected in these two cell types with addition of 10 ng/ml (F and I) of TGF-β. Bar = 20 μM

 doi:10.20944/preprints201905.0171.v1

2.2. Signaling pathways triggered by TGF-β stimulation.

The discrepancy in response to TGF-β stimulation led us to investigate whether the distinct modulation of FN profile between CFs, L6E9 skeletal myoblasts and CMs could be related to different signaling pathways triggered in the ECM regulation process. Thus, the classic and alternative TGF-β signaling pathways were evaluated in all cell types after cytokine treatment, using CM cultures as reference. Comparing the baseline response without TGF-β stimulus, L6E9 SMAD2 phosphorylation (PS2) was 5-fold higher than CM, while CF displayed 1.8-fold the PS2 levels of CM (Fig. 2A). Analysis of SMAD pathway revealed that following stimulation of skeletal myoblasts with 1 and 10 ng/ml of TGF-β, respectively, 2.1- and 2.9-fold increases in levels of PS2 in L6E9 skeletal myoblasts were observed, compared to untreated L6E9 cultures (Fig. 2A). The kinetics of TGF-β treatment of CFs revealed a 40% increase in PS2 levels after stimulation with 1ng/ml TGF-β, while with 10 ng/ml stimulation a maximum level of 69% increase was attained (Fig. 2A). Interestingly, L6E9 skeletal myoblasts were more susceptible to cytokine stimulation, presenting levels of PS2 10 to 13-fold higher than CM and 4-fold higher than CFs at the TGF-β concentrations analyzed. CF also presented more PS2 activation than CM, achieving increases of 2.5 and 2.7-fold above CM cultures when stimulated with 1 ng/ml and 10 ng/ml of TGF-β, respectively (Fig. 2A). CMs exhibit increase in PS2 level only after high doses of TGF-β (10 ng/ml) (Fig. 2A).

In parallel, we also evaluated the non-canonical p38 MAPK phosphorylation (phospho-p38MAPK, P-p38) pathway in CFs, CMs and L6E9 skeletal myoblasts after 1 h treatment with TGF-β (1-10 ng/ml). L6E9 skeletal myoblasts also showed P-p38 levels 80% higher than CM and 3.7-fold higher than CF at the baseline. L6E9 also showed increased sensitivity to TGF-β compared to CMs and CFs, reaching 2 and 4.7-fold increases in CM and CF levels, respectively, after TGF-β treatment (Fig. 2B). An increase in phospho-p38MAPK levels was observed in CF cultures stimulated with TGF-β, reaching a maximum of 45% increase in concentration at 10 ng/ml (Fig. 2B). In contrast, a 37% p38MAPK activation was noticed in CMs stimulated only with 10 ng/ml of TGF-β. In all concentrations of TGF-β (1-10 ng/ml), the phospho-p38MAPK levels in CF were significantly lower than in CMs and L6E9 (Fig. 2B). The addition of 1 ng/ml of TGF-β to L6E9 skeletal myoblasts resulted in a 1.2-fold increase of phospho-p38MAPK which remained constant after treatment with higher doses of TGF-β (Fig. 2B). In contrast, even though the response of L6E9 and CM to the cytokine stimulus was similar, with a rise in the range of 20-35%, TGF-β-treated CMs did not reach levels of phospho-p38MAPK comparable to the profile of stimulated L6E9 skeletal myoblasts even after high doses of cytokine treatment.

Preprints (www.preprints.org) | NOT PEER-REVIEWED | Posted: 14 May 2019 doi:10.20944/preprints201905.0171.v1

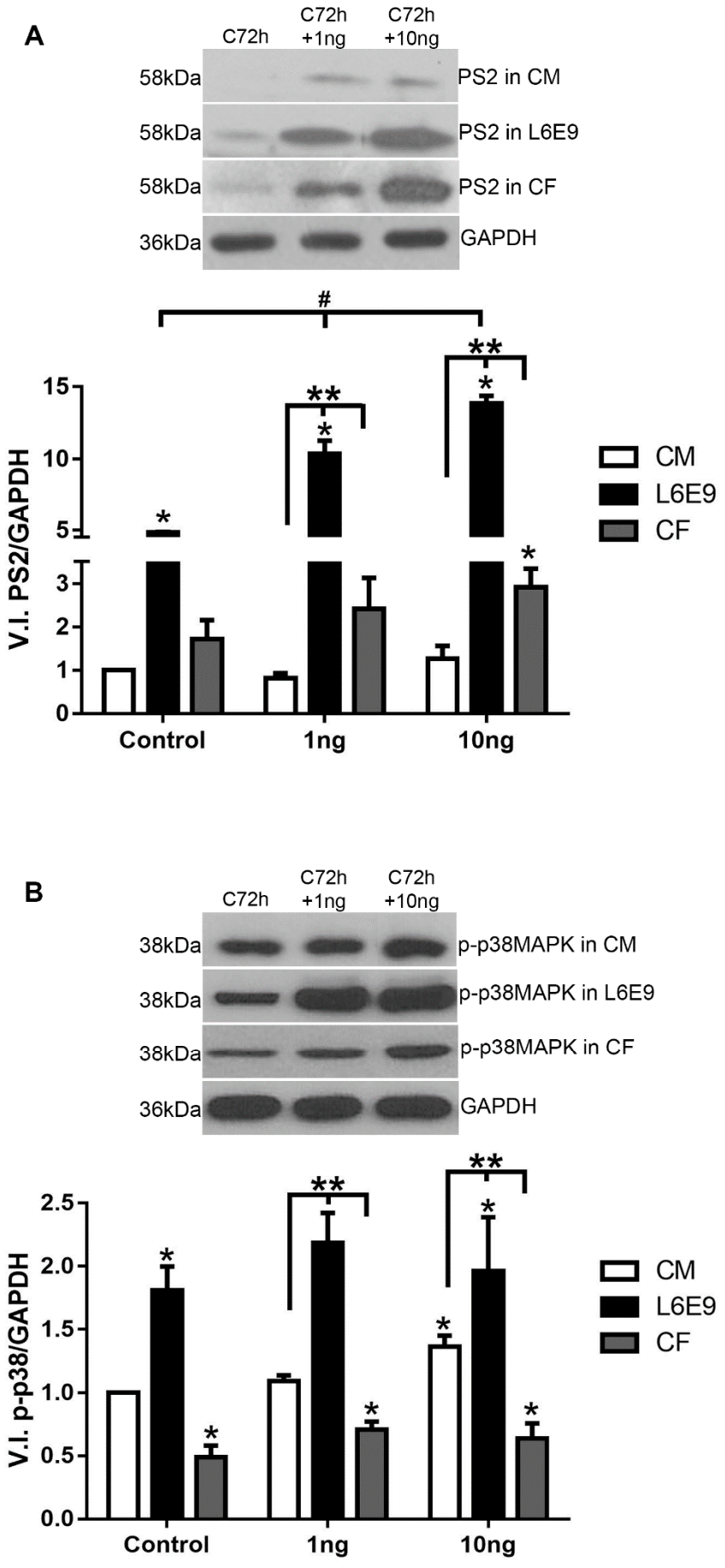

Preprints (www.preprints.org) | NOT PEER-REVIEWED | Posted: 14 May 2019 doi:10.20944/preprints201905.0171.v1

Figure 2 – Phosphorylated SMAD 2 and p38MAPK detection in normal cultures. (A) Comparison of PS2 detection of CM, skeletal myoblasts L6E9 and CF treated with TGF-β (1-10ng/ml) per 1 h. PS2 basal levels in L6E9 skeletal myoblasts and CF were significantly greater than CM. After the addition of TGF-β, PS2 remains significantly higher L6E9 and CF in relative to CM. L6E9 skeletal myoblasts respond to TGF-β stimulus in a dose dependent manner. CF shows a slight level of PS2 increase. * $p \leq 0.05$ compared to CM; ** $p \leq 0.05$ compared with CM in a different concentration; # $p \leq 0.05$ compared with L6E9 control. N = 3 **(B)** Comparison of p-p38MAPK detection of CM, skeletal myoblasts L6E9 and CF treated with TGF-β (1-10ng/ml) per 1 h. L6E9 skeletal myoblasts present a high level of p38MAPK phosphorylation when compared with CM. When CM was compared with CF, a higher p-p38MAPK phosphorylation after stimulation with TGF-β (1-10 ng/ml) was observed. * $p \leq 0.05$ compared to CM and ** $p \leq 0.05$ compared with CM in a different concentration. N = 3.

2.3. Differential fibronectin expression induced by T cruzi infection and TGF-β stimulation.

With the knowledge of the differential modulation in FN expression and the distinct activation of TGF-β–dependent signaling pathways (PS2 and p38) in the different cell types, we next sought to evaluate the response of these cells to *T. cruzi* infection. Thus, we evaluated the levels of FN expression in CFs and L6E9 skeletal myoblasts late in *T. cruzi* infection (72 h). Initially, the FN expression of CFs and L6E9 skeletal myoblasts cultures were analyzed after 48 h-treatment with TGF-β (1-10 ng/ml) by Western blot. Our results showed increased FN expression in both cell cultures at all TGF-β concentrations analyzed, but CFs were more responsive to cytokine stimulation (Fig. 3). L6E9 skeletal myoblasts showed a dose-dependent response with significant increases in FN expression ranging from 3- to 5.5-fold at different concentrations of TGF-β (1 to 10 ng/ml) (Fig. 3A). The highest FN increase was observed in CFs, with a 6.9-fold increase at 1 ng/ml, and 9.4-fold increase at 10 ng/ml, while L6E9 skeletal myoblasts reached a maximum of 5.5-fold enhancement at 10 ng/ml (Fig. 3).

Next, we analyzed the expression of FN in L6E9 and CFs infected by *T. cruzi* (72 h). Interestingly, *T cruzi* infection induced a differential response on FN expression in L6E9 skeletal myoblast and CF cultures (Fig. 3). Infected L6E9 skeletal myoblasts showed a significant 82% reduction in FN expression while FCs demonstrated a 5-fold up-regulation in the expression of this ECM component (Fig. 3). Although cytokine treatment stimulated a significant increase in FN expression in *T. cruzi*-infected L6E9 skeletal myoblasts, as compared to non-stimulated infected cells, FN expression levels were significantly down-regulated in comparison to stimulated control cells (Fig. 3A). Significant reductions of 67% and 45% in FN expression were demonstrated in *T cruzi*-infected L6E9 stimulated with 1 and 10 ng/ml TGF-β, respectively, compared to uninfected cultures. In contrast, *T. cruzi*-infected and stimulated CF

 doi:10.20944/preprints201905.0171.v1

cultures were not responsive to TGF-β stimulation, even at high concentrations of the cytokine (10 ng/ml), maintaining FN levels similar to control (Fig. 3B). In CF cultures with a high degree of infection, even treated with TGF-β, reductions of 38% (1 ng/ml) and 48% (10 ng/ml) in FN expression were observed when compared to their normal treated pairs (Fig. 3B).

Preprints (www.preprints.org) | NOT PEER-REVIEWED | Posted: 14 May 2019 doi:10.20944/preprints201905.0171.v1

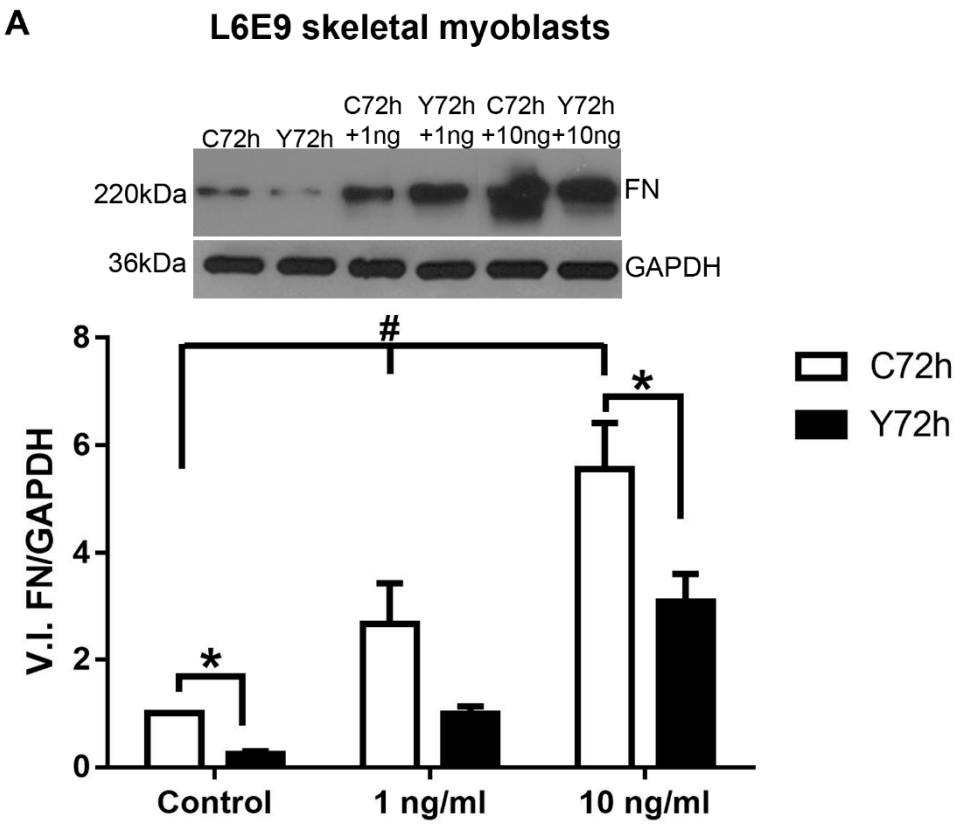

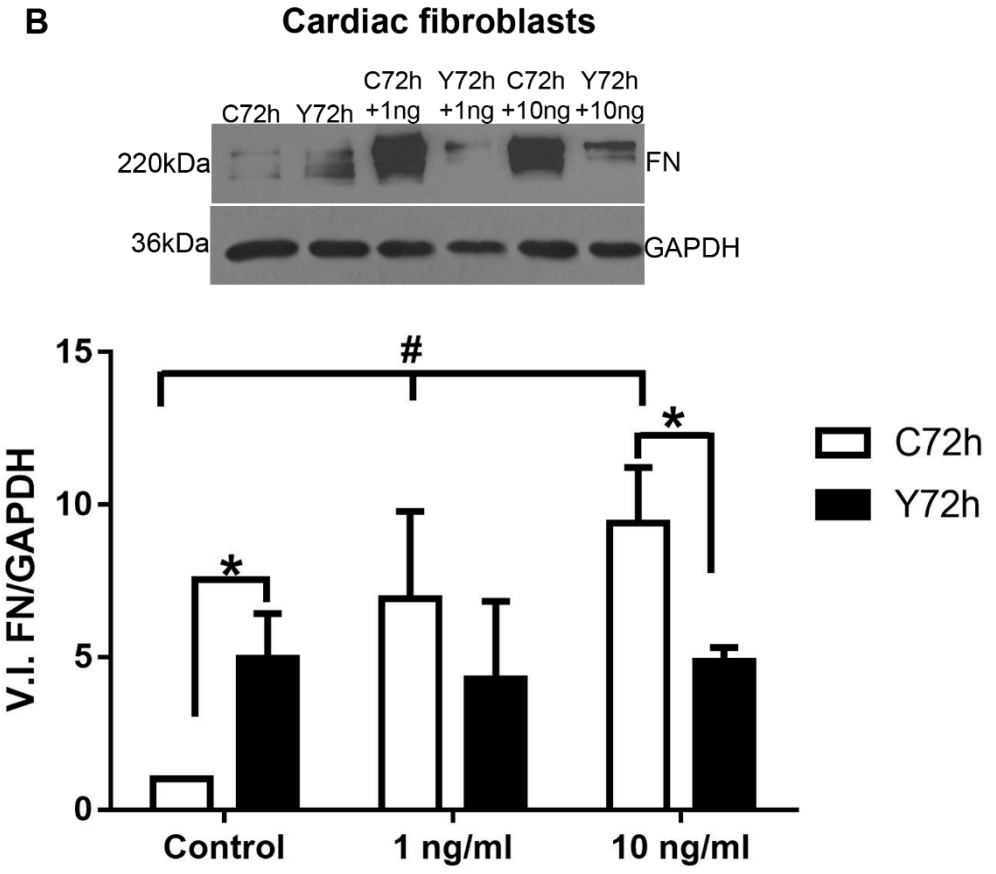

Preprints (www.preprints.org) | NOT PEER-REVIEWED | Posted: 14 May 2019 doi:10.20944/preprints201905.0171.v1

Figure 3 – Fibronectin expression in skeletal myoblasts L6E9 and cardiac fibroblasts treated with TGF- β. (A) In normal cultures, treatment with 1 ng/ml TGF-β for 48 h triggers the increase of FN expression in skeletal myoblasts L6E9, in a dose dependent manner after the addition of 1 and 10 ng/ml TGF-β. In L6E9 skeletal myoblasts infected with *T. cruzi* (72h), and treated with TGF-β (1 and 10 ng/ml) was observed an increase of FN expression when compared with infected untreated but there is a reduction in the FN expression when compared with uninfected cultures even after treatment with TGF-β (1 and 10 ng / ml). *p ≤ 0.05 compared to uninfected pairs; # p ≤ 0.05 compared to untreated control and uninfected; N = 4**. (B)** Normal CF was treated with TGF-β (1 and 10 ng/ml), showed an increase of FN expression according to the dose administered. In CF infected and untreated, there is an increase in the FN expression when compared with their normal counterparts. In CF infected and treated with TGF-β (1 and 10 ng/ml), a reduction of FN expression was observed when compared with their treated pairs. * p ≤ 0.05 compared to uninfected pairs and # p ≤ 0.05 compared with control uninfected and untreated. N = 3.

2.4. Regulation of fibronectin fibrillar network assembly by T. cruzi infection

The FN distribution in the extracellular matrix of L6E9 skeletal myoblasts and CF infected with *T. cruzi* and treated with TGF-β per 48h was evaluated by indirect immunofluorescence. Highly infected L6E9 skeletal myoblasts (Fig. 4C-F) and CF (Fig. 5C-F) cultures treated with TGF-β (1 and 10 ng/ml) showed a general increase in FN fibrils in the culture compared with the untreated controls (Fig. 4A-B and Fig. 5A-B). However, the FN increase was localized in adjacent non-infected cells, while highly infected cells displayed a reduction in FN distribution even after addition of high doses of TGF-β (1-10 ng/ml (Fig. 4C-F and Fig. 5C-F) compared to untreated controls. In both cell types, the remaining FN expression was redistributed, being seen along the borders of the infected cells instead of as the widespread fibrils observed in uninfected controls (Fig. 4 and Fig. 5).

Preprints (www.preprints.org) | NOT PEER-REVIEWED | Posted: 14 May 2019 doi:10.20944/preprints201905.0171.v1

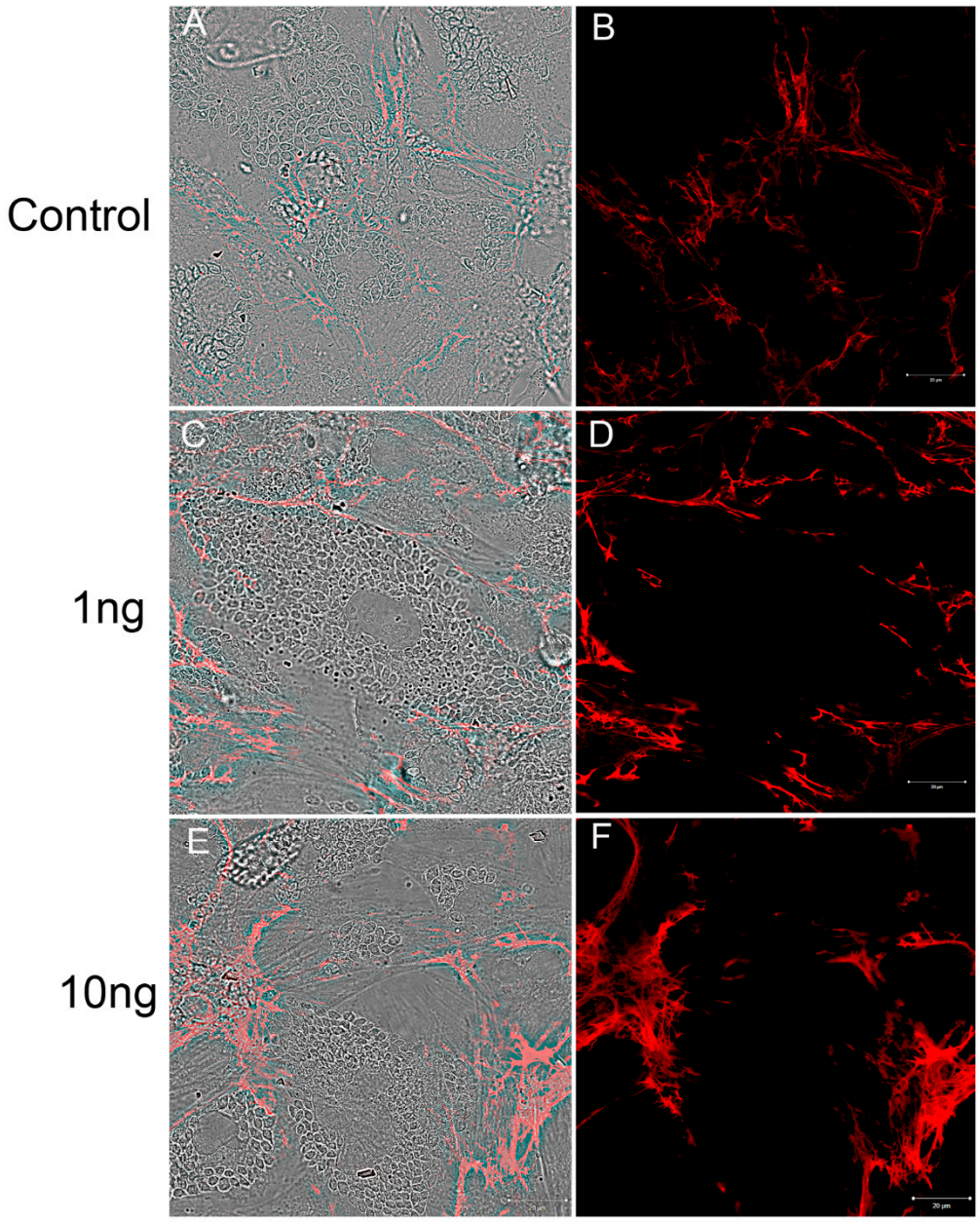

Figure 4 - Distribution of fibronectin in skeletal myoblasts L6E9 infected with *T. cruzi* and treated with TGF-β. L6E9 skeletal myoblasts (A-B) reduced FN after 72 h of *T. cruzi* infection in cells with intracellular parasites (*). The treatment in skeletal myoblasts L6E9 with 1 ng/mL (C-D), 5 ng/mL (E-F) or 10 ng/mL (G-H) of TGF-β induces a FN expression increase only in uninfected areas in this culture. Differential interference contrast (DIC) was used to label the intracellular parasites in the host cells. Bar = 20 μM

Preprints (www.preprints.org) | NOT PEER-REVIEWED | Posted: 14 May 2019 doi:10.20944/preprints201905.0171.v1

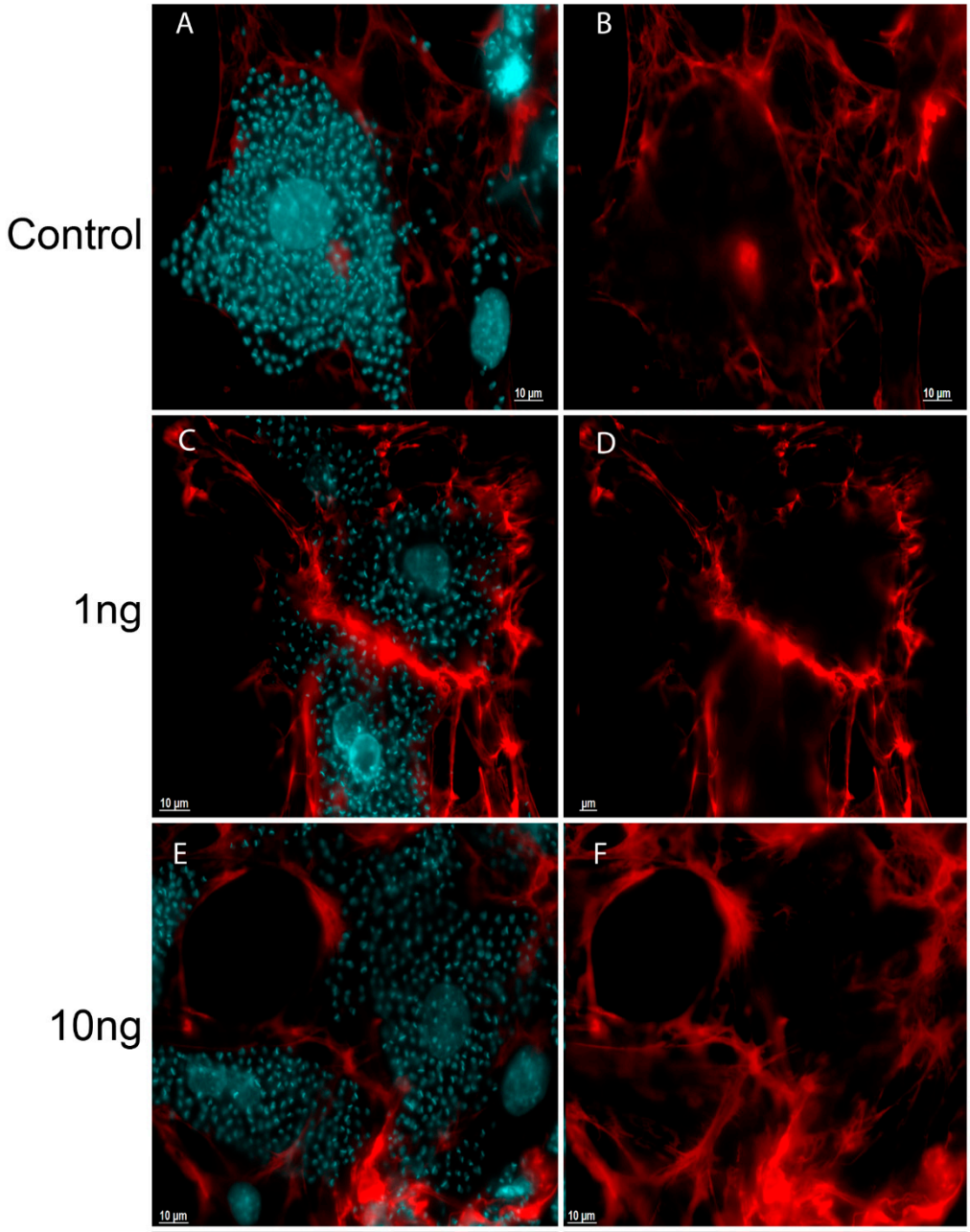

Figure 5 - Distribution of fibronectin in cardiac fibroblasts infected with *T. cruzi* and treated with TGF-β. FN in normal CF (A-B) and infected with *T. cruzi* (C-D). CF infected with *T. cruzi* showed a reduction of FN expression after 72 h of *T. cruzi*. Normal cardiac fibroblasts showed a higher FN expression after treatment with 1 ng/ml (E-F) and 10 ng/ml (I-J) of TGF-β in ECM. CF infected and treated with 1 ng/mL (G-H), and 10 ng/mL (K-L) presented a reduction in FN expression in this culture. DAPI (blue) was used to label the nucleus of the host cell and kinetoplast of intracellular parasites. Bar = 20 µM

 doi:10.20944/preprints201905.0171.v1

348 *2.5. Signaling pathways involved in ECM modulation triggered by T. cruzi cardiac*
349 *fibroblast infection*

350 The association of fibroblasts, the effector cells of fibrosis, with relative
351 down-regulation of FN expression in *T. cruzi*-infected cells after TGF-β
352 stimulation, led us to evaluate in detail the regulation of the signaling pathways
353 involved in ECM modulation. We analyzed the activation profiles of PS2, p-p38
354 MAPK and p-c-Jun signaling pathways in uninfected and *T. cruzi*-infected CFs
355 (72 h) subjected or not to stimulation with 10 ng/ml of TGF-β. A 59% reduction
356 in PS2 activation was evidenced in the infected CF cultures when compared to
357 their uninfected counterparts (Fig. 6A). Both uninfected and *T. cruzi*-infected CF
358 cultures were stimulated by the cytokine treatment. Addition of exogenous TGF-
359 β induced a significant 4.6-fold increase in PS2 activation of *T. cruzi*-infected FC
360 cultures compared to unstimulated infected cultures (Fig. 6A). However, a 28%
361 reduction in the activation of the SMAD2 pathway was evidenced when
362 compared to PS2 phosphorylation levels of the uninfected and TGF-β stimulated
363 culture (Fig. 6A). As expected, an inhibition of PS2 activation was revealed after
364 treatment of cultures with the specific pharmacological inhibitor SB431542
365 (ALK5 signaling inhibitor), reaching levels similar to controls (Fig. 6A).

366 Interestingly, high activation of p38 MAPK was revealed in CFs infected
367 with *T. cruzi* as compared to uninfected cultures, achieving a significant 54%
368 increase in the activation of this pathway. The addition of 10 ng/ml of TGF-β
369 induced a rise in the p38 MAPK phosphorylation in uninfected and infected CF
370 cultures, but its activation was 78% higher in infected cultures. SB431542
371 treatment prior to TGF-β stimulation led to a reduction of p38 MAPK
372 phosphorylation in both conditions (Fig. 6B).

373 Up-regulation of c-jun signaling pathway was also induced by *T. cruzi*
374 infection, showing a significant 1.98-fold increase of c-Jun phosphorylation
375 compared to uninfected CFs (Fig. 6C). Although 25% activation of c-Jun pathway
376 was observed in stimulated uninfected cells, the increase in phosphorylated c-
377 Jun levels in stimulated *T. cruzi*-infected CFs exceeded this value by 35%.
378 SB431542 also prevented c-Jun phosphorylation in uninfected and *T. cruzi*-
379 infected CF cultures.

380

381

Preprints (www.preprints.org) | NOT PEER-REVIEWED | Posted: 14 May 2019 doi:10.20944/preprints201905.0171.v1

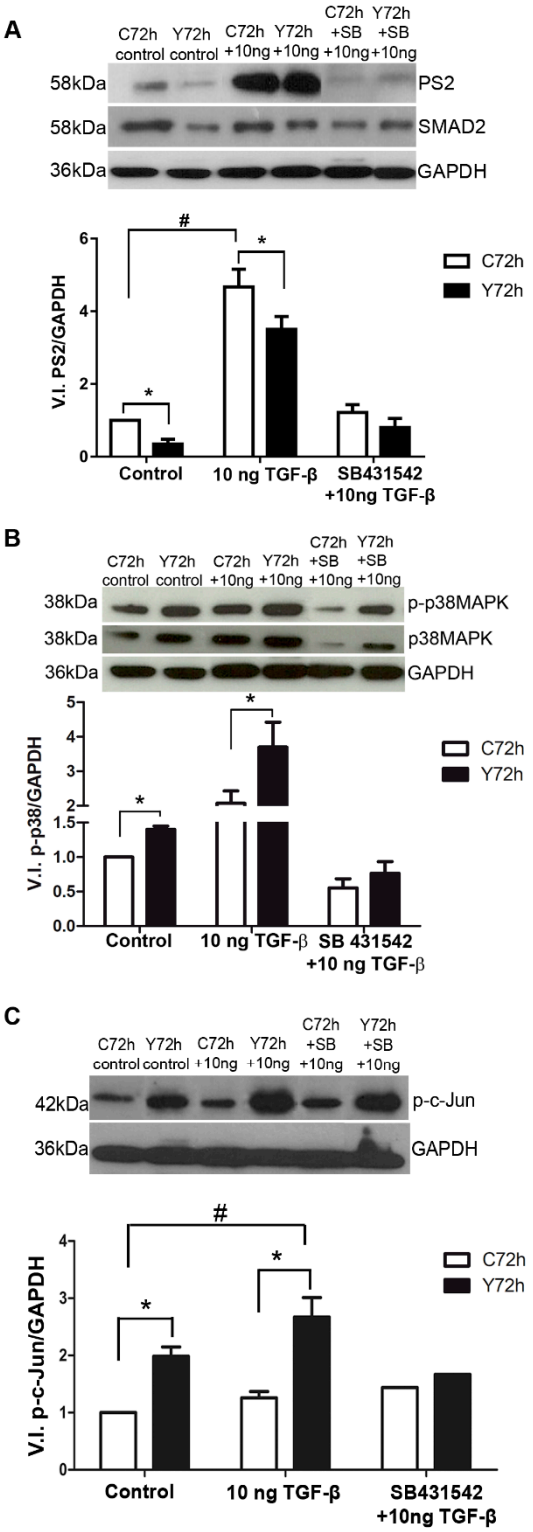

Figure 6 - PS2, p-p38 MAPK and p-c-Jun detection in normal and infected cardiac fibroblasts with *T. cruzi*. (A) PS2 detection. Normal CF showed an increase of SMAD2 phosphorylation when treated with 10 ng/ml of TGF-β. Infected CF were unable to trigger the classical signaling pathway even when was treated with 10 ng/ml, compared to the uninfected pair. The SB431542

Preprints (www.preprints.org) | NOT PEER-REVIEWED | Posted: 14 May 2019 doi:10.20944/preprints201905.0171.v1

inhibitor prevented SMAD 2 phosphorylation in CF cultures after stimulation with TGF-β. **(B) Phosphorylated p38 MAPK detection.** In normal CF treated with 10 ng/ml of TGF-β an increase of p38MAPK phosphorylation detection was observed. *T. cruzi* infection does not result in significant differences in p38 MAPK phosphorylation, although there was a tendency to an increase in this signaling pathway. After addition of 10 ng/ml of TGF-β, the signaling pathway was triggered in CF. The inhibitor SB431542 prevented the p38 MAPK phosphorylation in both normal and infected CF treated with 10 ng/ml TGF-β. **(C) Phosphorylated c-Jun detection.** Note that infection by *T. cruzi* leads to an increase c-Jun signaling pathway. The addition of TGF-β in normal cultures resulted in 25% an increase in c-Jun detection. The increase triggered by the infection remains and is enhanced by treatment with TGF-β. * $p \leq 0.05$ compared their control pairs.

2.6. Induction of cardiac fibroblast proliferation by T. cruzi infection and TGF-β stimulation

To evaluate whether *T. cruzi* infection and TGF-β play a role in the proliferation of CF, these cells were infected with *T. cruzi* and treated for 48 h with different concentrations of TGF- β (1-10 ng/mL). Interestingly, *T. cruzi* infection augmented CF proliferation by 37% as compared to uninfected cells. Both uninfected and *T. cruzi*-infected cultures showed similar response in the induction of CFs proliferation after stimulation with TGF-β. Two-and-a-half-fold higher levels in cell proliferation profiles were revealed from the stimulation of 10 ng/ml TGF-β in both uninfected and *T. cruzi*-infected cultures (Fig. 7).

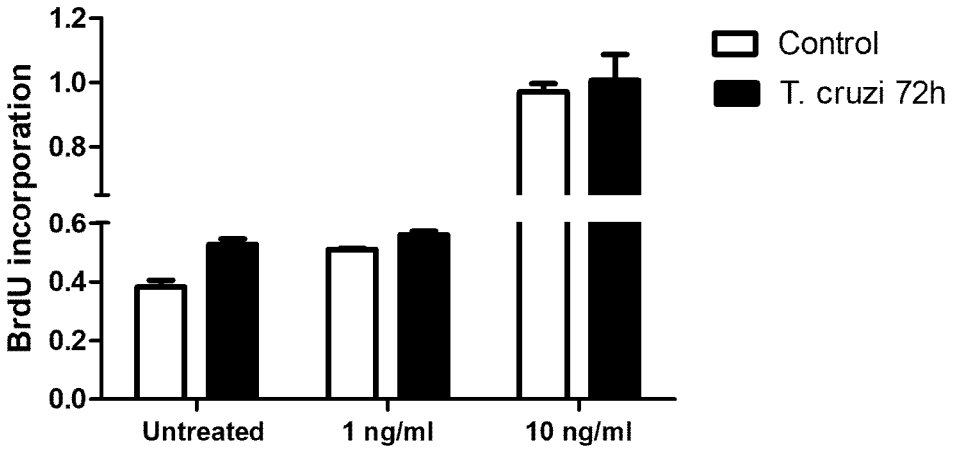

Figure 7 - Cardiac fibroblast proliferation treated with TGF-β. Cardiac fibroblasts treated with different concentrations of TGF-β (1 and 10 ng/mL) showed a high proliferation of cardiac fibroblasts in a dose dependent manner when compared with CF untreated. *$p \leq 0.05$ compared to CF untreated.

 doi:10.20944/preprints201905.0171.v1

3. Discussion

Cardiac fibrosis is a major feature of cardiomyopathy, increasing the deposition and accumulation of extracellular matrix proteins in the myocardium. TGF-β is a pro-fibrogenic cytokine and exerts a significant role in the heart as a regulator of components of ECM and is implicated in the genesis of cardiac fibrosis in Chagas disease [30].

In this study, FN expression and its distribution in ECM were analyzed in normal and *T. cruzi*-infected CF and L6E9 skeletal myoblasts treated with TGF-β (1-10 ng/ml). Also, the roles of classical and alternative TGF-β signaling pathways in the FN modulation in ECM in CF were investigated. Our data revealed that CF and L6E9 skeletal myoblasts showed an increase of FN starting in low concentrations of TGF-β (1-10 ng/ml). In contrast, normal cardiomyocytes displayed ECM stimulus only when treated with 10 ng/ml, similar to results previously reported by our group [34]. The differences observed in ECM expression in the different cell types could be explained by distinctive expression of TGF-β receptors, such as endoglin, an auxiliary type III TGF-β receptor that controls ECM expression in response to TGF-β [40]. Skeletal muscle cells do not have endoglin in their surface [41]. In CF, endoglin is constitutively expressed and is critical for TGF-β1 signaling, also modulating type I collagen synthesis in these cells [42]. Expression of endoglins, poorly understood in cardiomyocytes, occurs during the formation of the heart in the embryonic development, mainly in endothelial cells [43].

L6E9 skeletal myoblasts infected with *T. cruzi* showed a reduction of FN expression even after treatment with higher doses of TGF-β. In contrast, in CF, the overall measurement of the culture by Western blot showed an increase of FN, while immunofluorescence demonstrates that highly infected cells presented a redistribution of FN to the borders of the cell. In both cases, the parasite may be directly modulating the synthesis, secretion and organization of matrix proteins. In the case of CF, *T. cruzi* seems to be preventing the cell response to exogenous TGF-β stimulus. Evidence from the literature supports this idea, since a secreted/released factor from *T. cruzi* is capable of repressing CTGF/CCN2 expression in response to TGF-β in dermal fibroblasts, an effect also observed in the down-regulation of fibrogenic genes after infection [44]. The localized FN reduction and matrix delocalization in *T. cruzi*- infected L6E9 myoblasts and CF can also be associated with the actin cytoskeleton breakdown caused by the infection, which prevents both the anchoring of FN to integrins on the cell surface and the organization of FN matrix [45,46]. Previous work from our group has also shown a disorganization of the TGF-β receptor type II cell surface distribution induced by *T. cruzi* in cardiac fibroblast-containing primary cardiomyocyte cultures, which is associated with a lower global PS2 signaling response to exogenous TGF-β [47]. Furthermore, *T. cruzi* infection induced a significant reduction in the global levels of mRNA in the cytoplasm of host cell concomitant with the amastigote proliferation in primary cardiomyocyte cultures

 doi:10.20944/preprints201905.0171.v1

that also contained CF [48], suggesting that the intracellular multiplication of *T. cruzi* can affect the mRNA stability in the host, an effect that could result in reduced levels of protein synthesis.

In cardiac cultures infected with *T. cruzi*, different cytokines and chemokines such as TNF-α, IL-1β and iNOS are secreted in response of the infection [49]. The increase of FN expression in CF infected cultures suggests that the cellular stress against infection causes a release of cytokines like TNF-α, and that adjacent uninfected cells of the infected culture receive cytokine stimulus together with TGF-β, potentiating and modulating the synthesis and release of FN in the ECM. It was observed that in cardiac fibrosis, TNF-α may be involved in excessive accumulation of ECM in the myocardium [50]. Furthermore, mixed cultures containing cardiomyocytes and CF showed an increase in FN in response to stimulation with TNF-α [34].

Our results demonstrated that CF and skeletal L6E9 myoblasts showed higher SMAD2 phosphorylation than CM after TGF-β stimulation. However, p38 MAPK levels were higher in CM and skeletal L6E9 myoblasts when compared with CF. The differences in signaling responses can also be caused by differences in TGF-β receptor expression between the different cell types, including endoglins, as discussed above. In addition, in cardiac tissue, p38 MAPK signaling pathway is a dominant response to injury, leading to cardiomyocyte hypertrophy, through further activation of MKK3 and MKK6 [51]. Our data show that p38 MAPK detection was higher in cardiomyocytes than CF, suggesting that the p38 MAPK pathway may be resulting in hypertrophy rather than fibrosis in cardiomyocytes.

Our data showed that PS2 levels were reduced in *T. cruzi*-infected CF cultures after the addition of TGF-β (10 ng/ml) when compared to uninfected controls. The presence of the intracellular parasite in CF may modulate the classical signaling pathway and prevent the signal transduction to the nucleus. Studies in cardiomyocyte cultures showed that *T. cruzi* uptakes TGF-β for multiplication and development in the host cell, using it for its own cycle [25]. Also, the secreted factor from *T. cruzi* that inhibits TGF-β response in dermal fibroblasts [44] might also be disrupting SMAD signaling in CF.

We demonstrated an increase of p38MAPK phosphorylation in CF after *T. cruzi* infection and treatment with TGF-β. The p38 MAPK phosphorylation can modulate the deposition of ECM proteins in infected CF and might be a candidate for intervention against Chagas disease fibrosis. In *T. cruzi*-infected macrophage cultures, the exogenous addition of cruzipain, the most abundant cysteine protease of *T. cruzi*, and the JNK pathway inhibitor, SP600125, induces triggering and amplification of the p38MAPK signal in this cell type, favoring survival and amplification of the parasite in macrophages [52]. In other models of cardiomyopathy, p38 MAPK also was proven to be a critical pathway for fibrosis, since conditional knock-out of the p38α gene, *Map14k*, in cardiac

 doi:10.20944/preprints201905.0171.v1

fibroblasts blocked myofibroblast differentiation after ischemic injury and led to reduced heart fibrosis [53].

Our data revealed that *T. cruzi* infection increases c-Jun phosphorylation in CF. When TGF-β binds to it specific receptor, a rapid c-Jun activation occurs, depending on the cell type, leading to SMAD3 phosphorylation. Therefore, c-Jun signaling may increase the classical signaling pathway through SMAD3 phosphorylation [54,55]. In *T. cruzi*-infected macrophage cultures, an increase in c-Jun phosphorylation was similarly observed [52]. Likewise, significant up-regulation of c-Jun was detected in early *T. cruzi* infection of primary human colonic epithelial cells by phosphoproteomics and Western blot [56]. In addition, primary cultures of cardiac myocytes displayed an increase in nuclear translocation of JunB up to 2 h after *T. cruzi* infection [57]. These data demonstrate that the parasite has an important role in the activation of c-Jun in different cell types and also in CF cultures, where an increase in c-Jun phosphorylation triggered by infection is observed independent of TGF-β treatment, suggesting that c-Jun as a candidate target for intervention against Chagas disease fibrosis in the heart.

To investigate if FN increase resulting from *T. cruzi* infection was caused by CF proliferation stimulated by the parasite, we measured BrdU incorporation in *T. cruzi*-infected CF cultures treated with different concentrations of TGF-β. Our results showed that *T. cruzi* infection and TGF-β promoted the proliferation of cardiac fibroblasts, with TGF-β response being observed in a dose-dependent manner, an effect consistent with fibrosis development in the myocardium in CD. Different sources of evidence show that *T. cruzi*-derived molecules can modulate fibroblast proliferation. Conditioned media from *T. cruzi*-infected cultures and amastigote extracts stimulated [^{3}H]thymidine incorporation in human dermal fibroblasts, although the authors were not able to identify which parasite molecule was responsible for this process [58]. More recently, recombinant *T. cruzi* calreticulin (TcCRT) was shown to induce fibroblast migration in scratch plate assays and increase proliferation of human dermal fibroblasts three orders of magnitude more efficiently than the recombinant human calreticulin [59]. Thus, *T. cruzi* can potentially modulate cardiac fibroblast proliferation either by direct infection or through a paracrine effect of infected cells over uninfected cells, or possibly via the remaining antigens of dead parasites in the Chagas patient's cardiac tissue [60] acting through *T. cruzi* calreticulin. Cardiac fibroblast proliferation can be targeted for treatment, since tetrandrine, a drug used for cancer treatment, can inhibit the proliferation of cardiac fibroblasts induced by TGF-β [61], and potentially could be repurposed for treatment of cardiac fibrosis in Chagas Disease.

Altogether, our studies open new perspectives to understand the regulatory mechanisms of TGF-β in FN matrix in cardiomyocytes, cardiac fibroblasts and L6E9 myoblasts, and uncover new therapeutic targets against cardiac fibrosis in Chagas Disease.

Preprints (www.preprints.org) | NOT PEER-REVIEWED | Posted: 14 May 2019 doi:10.20944/preprints201905.0171.v1

4. Materials and methods

Primary cardiomyocyte culture

Primary cultures of cardiomyocytes and cardiac fibroblasts were performed using 18-day-old mouse embryos as previously described [62]. Cardiac fragments were dissociated in phosphate buffered saline (PBS; 137 mM NaCl, 2.7 mM KCl, 0.88 mM KH_2PO_4, 6.4 mM Na_2HPO_4, pH7.2) containing 0.025% trypsin and 0.01% collagenase (Worthington Co., Lakewood, NJ, USA) and plated into a 24-well plate (10^5 cells/ml) containing glass coverslips coated with 0.01% gelatin. Although cardiomyocytes constitute approximately 80% of the total cells, the culture still displayed myoblasts and fibroblasts. Cultures were cultivated in Dulbecco's modified Eagle medium (DMEM; Sigma Chemical Co, St. Louis, MO, USA) supplemented with 10% fetal bovine serum (FBS; Sigma), 2.5 mM $CaCl_2$, 1 mM L-glutamine and 2% chicken embryo extract and kept at 37 ºC in an atmosphere of 5% CO_2.

Cardiac fibroblasts and skeletal muscle myoblasts culture

Cardiac fibroblast (CF) cultures were purified from successive dissociations of mouse cardiac muscle cells primary cultures. Cells seeded in 25 cm^2culture flasks were grown in DMEM supplemented with 10% FBS, 2% chicken embryo extract, 2.5 mM $CaCl_2$, 1 mM L-glutamine and antibiotics and kept at 37 °C in 5% CO_2 atmosphere. Fibroblast purification was carried out by differential plating method and successive subculture based on the slower adhesion of cardiomyocytes to substrate and its susceptibility to sequential enzyme activity, respectively. Rat skeletal muscle myoblasts from L6E9 lineage were maintained in DMEM supplemented with 10% FBS, 1 mM L-glutamine. The cells were subcultured by the dissociation of confluent cultures with a solution of 0.025% trypsin and 0.01% EDTA in PBS. After dissociation, the isolated cells were counted and seeded at a density of 5 x 10^4 cells/well and 5 x 10^5 cells/dish in 24-well plates and 60 mm dishes, respectively.

Parasites and cell culture infection

Trypomastigotes of *T. cruzi*, Y strain, derived from Vero culture were used. Cardiac muscle cells, CF and skeletal myoblasts L6E9 were infected at a multiplicity of infection of 10 parasites/host cell (10:1) after 24 h of cultivation. The infection was interrupted after 72 h.

Treatment of cardiomyocytes, cardiac fibroblasts and skeletal myoblasts L6E9 with TGF-β

Normal and 24 h-infected cultures were washed with Ringer's solution to remove the FBS contained in the nutritive medium. The treatment was performed with recombinant TGF-β (R &D Systems, Minneapolis, MN, USA) diluted in DMEM supplemented with 0.1% FBS, 2.5 mM $CaCl_2$ and 2% L-glutamine. TGF-β was

 doi:10.20944/preprints201905.0171.v1

591 added at concentrations of 1, 5, 10 and 15 ng/ml after 24 h of cultivation. The cells
592 were fixed after 48 h of TGF-β treatment and 72 h of *T. cruzi* infection. For analysis
593 of signaling pathways, the treatment with recombinant TGF-β was performed for
594 1 h in the same concentrations, in normal and *T. cruzi*-infected cultures (72 h).
595
596 **Indirect Immunofluorescence**
597 Cardiomyocytes, CF and skeletal myoblasts L6E9, treated or not with TGF-β,
598 were fixed for 5 min at room temperature with 4% paraformaldehyde (PFA) in
599 PBS followed by washing in PBS. To block nonspecific reactions, monolayers
600 were washed (3 X 20 min) with PBS containing 4 % bovine serum albumin (BSA).
601 The cells were, then, incubated for 18 h at 4 °C with anti-fibronectin antibody
602 (1:400; Sigma Chemical Co.). After successive washes in PBS, the cultures were
603 incubated for 1 h at 37 °C with secondary anti-rabbit antibody TRICT-conjugated
604 (1:200; Sigma). For visualization of the nucleus, cells were stained with 4',6 -
605 diamidino -2- phenilyndole (DAPI; DNA dye) and, then, the coverslips were
606 mounted in 2.5% 1'4 - Diazabicyclo -(2.2.2)- octane (DABCO, Sigma Chemical
607 Co.) in PBS/ 50% glycerol and sealed with nail polish. The images were acquired
608 at the confocal laser scanning microscope Zeiss LSM 510 Meta.
609
610 **Protein extraction**
611 Cardiomyocytes, CFs and L6E9 skeletal myoblasts, treated or not with TGF-β,
612 were washed 3 times with cold PBS on ice. Then, the cells were scraped in lysis
613 buffer (50 mM Tris, 150 mM NaCl, 1% Triton X-100, pH 8.0) containing
614 phosphatase and protease inhibitors (PhosStop Roche Diagnostics), 1 mM EGTA,
615 1mg/ml pepstatin, 100 mg/ml PMSF, 1 μg/ml aprotinin and 2 mg/ml leupeptin).
616 After the lysis, electrophoresis sample buffer 5X was added (0.3 M Tris, 10% SDS,
617 0.125% Bromophenol Blue, 25% β-mercaptoethanol and 50% glycerol) and the
618 samples were heated to 100 °C for 5 min in a dry bath. After the samples cool
619 down to room temperature, the samples were stored at –20 °C. Before adding the
620 sample buffer, an aliquot of each sample was separated to quantify the total
621 protein amount using the Folin-Lowry method.
622
623 **Western Blot**
624 After the determination of protein concentration, 10 μg or 20 μg of total protein
625 extracts obtained from cardiomyocytes, CFs and skeletal myoblasts L6E9 normal
626 and infected, treated or not with TGF-β, were subjected to electrophoresis on 10%
627 and 12% of polyacrylamide gel containing SDS (SDS-PAGE). The electrophoretic
628 separated proteins were transferred to nitrocellulose membranes and incubated
629 for 1 h at 4 °C with blocking buffer consisting of 25 mM Tris, 150 mM NaCl and
630 0,05% Tween 20 (TBST), 5% non-fat dry milk (Molico) and 0.1% Tween 20. After
631 blocking, the membranes were incubated with anti-fibronectin antibody (1:5000;
632 Sigma Chemical Co.), anti-phosphorylated SMAD2 (1:2000; Millipore), anti-
633 phosphorylated p38 (1:1000; Cell Signaling) and anti-phosphorylated c-Jun

 doi:10.20944/preprints201905.0171.v1

(1:500; Millipore) for 18 h at 4 °C. Anti-GAPDH (1:50.000; RDI Fitzgerald) was used as internal control. The membranes were then washed with TBST and incubated for 1 h at room temperature with anti-rabbit or anti-mouse peroxidase conjugate (Pierce Biotechnology) diluted 1:20.000 and 1:30.000, respectively, in blocking buffer. The membranes were washed, and the peroxidase was revealed by chemiluminescence using the Super Signal West Pico (Pierce Biotechnology) kit. Densitometry of the resulting bands was performed with the Image J program (http://rsbweb.nih.gov/ij/).

Cardiac Fibroblasts Proliferation

CFs, plated in a density of 1.5 x 10^4 cells per well in a 96 well plates, were infected with *T. cruzi* (Y strain, 10 parasites/host cell), and after 24 h of infection the cultures were treated with 1, 5 and 10 ng/ml of TGF-β per 48 h. Measurement of proliferation of CFs was performed using BrdU Cell Proliferation Kit (Millipore), according to manufacturer's instructions. Briefly, after 48 h of treatment with TGF- β and 72 h of *T. cruzi* infection, the cultures were incubated with 20 μg/ml of 5-bromo-2'-deoxiuridin (BrdU), allowing its incorporation in proliferating cells for 2 h. Cells were fixed and the DNA was denatured with the solution provided by the kit for 30 min at room temperature. After washing, the BrdU-labeled DNA was detected by the monoclonal anti-BrdU antibody for 1 h at room temperature. The plate was washed, and the antigen-antibody complex was revealed by addition of peroxidase-conjugate goat anti-mouse IgG, antibody and TMB as peroxidase substrate. The reaction was stopped with acid Stop Solution and the colorimetric reaction was read in a M2 Spectramax Plate Reader (Molecular devices) at λ450 nM.

Supplementary Materials: Supplementary materials can be found online.

Author Contributions: Conceptualization, Calvet C.M.; methodology, Calvet C.M., Pereira M.C.S.; investigation, Calvet C.M., Silva T.A., Ferreira, L.F.C.; resources, Calvet C.M., Pereira M.C.S.; data curation, Calvet C.M., Silva T.A., Ferreira, L.F.C.; writing—original draft preparation, Silva T.A.; writing—review and editing, Calvet C.M., Pereira M.C.S. ; visualization, Calvet C.M., Silva T.A.; supervision, Calvet C.M., Pereira M.C.S.; funding acquisition, Calvet C.M., Pereira M.C.S.

Funding: This research was funded by by research funds from the Oswaldo Cruz Institute of the Oswaldo Cruz Foundation (Fiocruz), Programa Estratégico de Apoio à Pesquisa em Saúde (Papes VI)/Conselho Nacional de Desenvolvimento Científico e Tecnológico (CNPq), Brazil (grant 421856/2017-3 and 424015/2018-8 to M.C.S.P.), Fundação de Amparo à Pesquisa do Estado do Rio de Janeiro (FAPERJ) (grant E-26/010.001548/2014 and E-26/110.553/2014 to M.C.S.P. and E26/110.817/2009 to C.M.C) and Coordenação de Aperfeiçoamento de Pessoal de Nível Superior - Brasil (CAPES) - Finance Code 001.

Acknowledgments: The authors acknowledge Liliane Batista de Mesquita and Alanderson Nogueira for technical support with cardiomyocyte and parasite culture; Pedro Paulo de A. Manso and Carlos Bizarro for confocal image acquisition; Potter Wickware for editorial assistance.

Conflicts of Interest: The authors declare no conflict of interest.

References

1. Chagas, C. Nova tripanozomiaze humana. *Mem. Inst. Oswaldo Cruz* **1909**, *1*, *no:2*, 0074–0276.
2. Moncayo, Á.; Silveira, A.C. Current epidemiological trends of Chagas disease in Latin America and future challenges: epidemiology, surveillance, and health policies. *Am. Trypanos. Chagas Dis.* **2017**, 59–88.
3. WHO Chagas Disease- factsheet. *Wkly. Epidemiol. Rec.* **2012**, 519–522.
4. Nunes, M.C.P.; Dones, W.; Morillo, C. a; Encina, J.J.; Ribeiro, A.L. Chagas disease: an overview of clinical and epidemiological aspects. *J. Am. Coll. Cardiol.* **2013**, *62*, 767–76.
5. Maldonado, I.R.S.C.; Ferreira, M.L.; Camargos, E.R.S.; Chiari, E.; Machado, C.R.S. Skeletal muscle regeneration and Trypanosoma cruzi-induced myositis in rats. *Histol. Histopathol.* **2004**, *19*, 85–93.
6. Rassi, A.; Marcondes de Rezende, J. American trypanosomiasis (Chagas disease). *Infect. Dis. Clin. North Am.* **2012**, *26*, 275–91.
7. Menezes Junior, A. da S.; Lopes, C.C.; Cavalcante, P.F.; Martins, E. Chronic Chagas Cardiomyopathy Patients and Resynchronization Therapy: a Survival Analysis. *Brazilian J. Cardiovasc. Surg.* **2018**, *33*, 82–88.
8. Benziger, C.P.; do Carmo, G.A.L.; Ribeiro, A.L.P. Chagas Cardiomyopathy: Clinical Presentation and Management in the Americas. *Cardiol. Clin.* **2017**, *35*, 31–47.
9. Rassi Jr, A.; Marin-Neto, J.A.; Rassi, A. Chronic Chagas cardiomyopathy: a review of the main pathogenic mechanisms and the efficacy of aetiological treatment following the BENznidazole Evaluation for Interrupting Trypanosomiasis (BENEFIT) trial. *Mem Inst Oswaldo Cruz Rio Janeiro* **2017**, *112*, 224–235.

10. Monteón, V.M.; Furuzawa-Carballeda, J.; Alejandre-Aguilar, R.; Aranda-Fraustro, A.; Rosales-Encina, J.L.; Reyes, P.A. American Trypanosomosis : In Situ and Generalized Features of Parasitism and Inflammation Kinetics in a Murine Model. *Exp. Parasitol.* **1996**, *83*, 267–274.
11. Fujiu, K.; Nagai, R. Fibroblast-mediated pathways in cardiac hypertrophy. *J. Mol. Cell. Cardiol.* **2014**, *70*, 64–73.
12. Deb, A.; Ubil, E. Cardiac fibroblast in development and wound healing. *J. Mol. Cell. Cardiol.* **2014**, *70*, 47–55.
13. Morikawa, M.; Derynck, R.; Miyazono, K. TGF- β and the TGF-β family: Context-dependent roles in cell and tissue physiology. *Cold Spring Harb. Perspect. Biol.* **2016**, *8*, a021873.
14. Araújo-Jorge, T.C.; Waghabi, M.C.; Hasslocher-Moreno, A.M.; Xavier, S.S.; Higuchi, M.D.L.; Keramidas, M.; Bailly, S.; Feige, J.-J. Implication of transforming growth factor-beta1 in Chagas disease myocardiopathy. *J. Infect. Dis.* **2002**, *186*, 1823–8.
15. Araújo-Jorge, T.C.; Waghabi, M.C.; Bailly, S.; Feige, J.-J. The TGF-β pathway as an emerging target for Chagas disease therapy. *Clin. Pharmacol. Ther.* **2012**, *92*, 613–621.
16. Zhao, B.; Chen, Y.-G. Regulation of TGF-β Signal Transduction. *Scientifica (Cairo).* **2014**, *2014*, 874065.
17. Akhurst, R.J.; Hata, A. Targeting the TGFβ signalling pathway in disease. *Nat. Rev. Drug Discov.* **2012**, *11*, 790–811.
18. Massagué, J. TGFβ signalling in context. *Nat. Rev. Mol. Cell Biol.* **2012**, *13*, 616–30.
19. Mu, Y.; Gudey, S.K.; Landström, M. Non-Smad signaling pathways. *Cell Tissue Res.* **2012**, *347*, 11–20.
20. Hall, B.S.; Pereira, M.A. Dual Role for Transforming Growth Factor ☒ - Dependent Signaling in Trypanosoma cruzi Infection of Mammalian Cells. **2000**, *68*, 2077–2081.
21. Ming, M.; Ewen, M.E.; Pereira, M.E.A.; Street, W. Trypanosome Invasion of Mammalian Cells Requires Activation of the TGFp Signaling Pathway. **1995**, *82*, 287–296.
22. Waghabi, M.C.; Keramidas, M.; Calvet, C.M.; Meuser, M.; Soeiro, M.D.N.C.; Mendonça-Lima, L.; Araújo-Jorge, T.C.; Feige, J.-J.; Bailly, S. SB-431542, a transforming growth factor β inhibitor, impairs Trypanosoma cruzi infection in cardiomyocytes and parasite cycle completion. *Antimicrob. Agents Chemother.* **2007**, *51*.
23. Waghabi, M.C.; Keramidas, M.; Feige, J.-J.; Araujo-Jorge, T.C.; Bailly, S. Activation of transforming growth factor beta by Trypanosoma cruzi. *Cell. Microbiol.* **2005**, *7*, 511–7.
24. Waghabi, M.C.; Coutinho-Silva, R.; Feige, J.-J.; Higuchi, M.D.L.; Becker, D.; Burnstock, G.; Araújo-Jorge, T.C. Gap junction reduction in

766 cardiomyocytes following transforming growth factor-beta treatment and
767 Trypanosoma cruzi infection. *Mem. Inst. Oswaldo Cruz* **2009**, *104*, 1083–
768 1090.
769 25. Waghabi, M.C.; Keramidas, M.; Bailly, S.; Degrave, W.; Mendonça-Lima,
770 L.; Soeiro, M.D.N.C.; Meirelles, M.D.N.L.; Paciornik, S.; Araújo-Jorge,
771 T.C.; Feige, J.J. Uptake of host cell transforming growth factor-beta by
772 Trypanosoma cruzi amastigotes in cardiomyocytes: potential role in
773 parasite cycle completion. *Am. J. Pathol.* **2005**, *167*, 993–1003.
774 26. Ferrão, P.M.; d'Avila-Levy, C.M.; Araujo-Jorge, T.C.; Degrave, W.M.;
775 Gonçalves, A.D.S.; Garzoni, L.R.; Lima, A.P.; Feige, J.J.; Bailly, S.;
776 Mendonça-Lima, L.; et al. Cruzipain Activates Latent TGF-β from Host
777 Cells during T. cruzi Invasion. *PLoS One* **2015**, *10*, e0124832.
778 27. Martin, D.L.; Postan, M.; Lucas, P.; Gress, R.; Tarleton, R.L. TGF-beta
779 regulates pathology but not tissue CD8+ T cell dysfunction during
780 experimental Trypanosoma cruzi infection. *Eur. J. Immunol.* **2007**, *37*,
781 2764–71.
782 28. Waghabi, M.C.; Coutinho, C.M.L.M.; Soeiro, M.N.C.; Pereira, M.C.S.;
783 Feige, J.; Keramidas, M.; Cosson, A.; Minoprio, P.; Leuven, F. Van; Arau,
784 T.C.; et al. Increased Trypanosoma cruzi Invasion and Heart Fibrosis
785 Associated with High Transforming Growth Factor β Levels in Mice
786 Deficient in α2 -Macroglobulin. *Infect. Immun.* **2002**, *70*, 5115–5123.
787 29. Rodrigues, D.B.R.; dos Reis, M.A.; Romano, A.; Pereira, S.A.D.L.; Teixeira,
788 V.D.P.A.; Tostes, S.; Rodrigues, V. In situ expression of regulatory
789 cytokines by heart inflammatory cells in Chagas' disease patients with
790 heart failure. *Clin. Dev. Immunol.* **2012**, *2012*, 361730.
791 30. Araújo-Jorge, T.C.; Waghabi, M.C.; Hasslocher-moreno, A.M.; Xavier, S.;
792 Higuchi, M.D.L.; Keramidas, M.; Bailly, S.; Feige, J. Implication of
793 Transforming Growth Factor – β1 in Chagas Disease Myocardiopathy. *J.*
794 *Infect. Dis.* **2002**, *186*, 1823–1828.
795 31. Ferreira, R.R.; de Souza, E.M.; de Oliveira, F.L.; Ferrão, P.M.; Gomes,
796 L.H.F.; Mendonça-Lima, L.; Meuser-Batista, M.; Bailly, S.; Feige, J.J.; de
797 Araujo-Jorge, T.C.; et al. Proteins involved on TGF-β pathway are up-
798 regulated during the acute phase of experimental Chagas disease.
799 *Immunobiology* **2016**, *221*, 587–94.
800 32. de Oliveira, F.L.; Araújo-Jorge, T.C.; de Souza, E.M.; de Oliveira, G.M.;
801 Degrave, W.M.; Feige, J.-J.; Bailly, S.; Waghabi, M.C. Oral administration
802 of GW788388, an inhibitor of transforming growth factor beta signaling,
803 prevents heart fibrosis in Chagas disease. *PLoS Negl. Trop. Dis.* **2012**, *6*,
804 e1696.
805 33. Bogoyevitch, M.A.; Boehm, I.; Oakley, A.; Ketterman, A.J.; Barr, R.K.
806 Targeting the JNK MAPK cascade for inhibition: Basic science and
807 therapeutic potential. *Biochim. Biophys. Acta - Proteins Proteomics* **2004**,
808 *1697*, 89–101.

34. Calvet, C.M.; Oliveira, F.O.R.; Araújo-Jorge, T.C.; Pereira, M.C.S. Regulation of extracellular matrix expression and distribution in Trypanosoma cruzi-infected cardiomyocytes. *Int. J. Med. Microbiol.* **2009**, *299*, 301–12.
35. Waghabi, M.C.; de Souza, E.M.; de Oliveira, G.M.; Keramidas, M.; Feige, J.-J.; Araújo-Jorge, T.C.; Bailly, S. Pharmacological inhibition of transforming growth factor beta signaling decreases infection and prevents heart damage in acute Chagas' disease. *Antimicrob. Agents Chemother.* **2009**, *53*, 4694–701.
36. Ferrão, P.; Nisimura, L.; Moreira, O.; Land, M.; Pereira, M.C.; de Mendonça-Lima, L.; Araujo-Jorge, T.; Waghabi, M.; Garzoni, L. Inhibition of TGF-β pathway reverts extracellular matrix remodeling in T. cruzi - infected cardiac spheroids. *Exp. Cell Res.* **2018**, *362*, 260–267.
37. Calvet, C.M.; Meuser, M.; Almeida, D.; Meirelles, M.N.L.; Pereira, M.C.S. Trypanosoma cruzi-cardiomyocyte interaction: role of fibronectin in the recognition process and extracellular matrix expression in vitro and in vivo. *Exp. Parasitol.* **2004**, *107*, 20–30.
38. Leask, A. TGFbeta, cardiac fibroblasts, and the fibrotic response. *Cardiovasc. Res.* **2007**, *74*, 207–12.
39. Ignotz RA, M.J. Cell adhesion protein receptors as targets for transforming growth factor-beta action. *Cell* **1987**, *51*, 189–197.
40. García-Pozo, L.; Miquilena-Colina, M.E.; Lozano-Rodríguez, T.; García-Monzón, C. Endoglin: structure, biological functions, and role in fibrogenesis. *Rev. Española Enfermedades Dig.* **2008**, *100*, 355–360.
41. Rodríguez-Barbero, A.; Obreo, J.; Álvarez-Muñoz, P.; Pandiella, A.; Bernabeu, C.; Lopes-Novoa, J.M. Endoglin Modulation of TGF-β induced collagen synthesis is dependent on ERK1 / 2 MAPK Activation. *Cell. Physiol. Biochem.* **2006**, *18*, 135–142.
42. Kapur, N.K.; Wilson, S.; Yunis, A. a; Qiao, X.; Mackey, E.; Paruchuri, V.; Baker, C.; Aronovitz, M.J.; Karumanchi, S.A.; Letarte, M.; et al. Reduced endoglin activity limits cardiac fibrosis and improves survival in heart failure. *Circulation* **2012**, *125*, 2728–38.
43. Nomura-Kitabayashi, A.; Anderson, G. a; Sleep, G.; Mena, J.; Karabegovic, A.; Karamath, S.; Letarte, M.; Puri, M.C. Endoglin is dispensable for angiogenesis, but required for endocardial cushion formation in the midgestation mouse embryo. *Dev. Biol.* **2009**, *335*, 66–77.
44. Mott, G.A.; Costales, J.A.; Burleigh, B.A. A soluble factor from Trypanosoma cruzi inhibits transforming growth factor-ß-induced MAP kinase activation and gene expression in dermal fibroblasts. *PLoS One* **2011**, *6*, e23482.
45. Melo, T.G.; Tucci, A.R.; Nogueira, A.R.; Meirelles, M.D.N.S.L.; Pereira, M.C.S. The involvement of FAK and Src in the invasion of cardiomyocytes by Trypanosoma cruzi. *Exp. Parasitol.* **2014**, *139*, 49–57.

46. Pereira, M.C. de S.; Costa, M.; Chagas Filho, C.; de Meirelles, M.D.N.S.L. Myofibrillar breakdown and cytoskeletal alterations in heart muscle cells during invasion by Trypanosoma cruzi: immunological and ultrastructural study. *J. Submicrosc. Cytol. Pathol.* **1993**, *25*, 559–569.
47. Calvet, C.M.; Silva, T.A.; De Melo, T.G.; De Araújo-Jorge, T.C.; De Souza Pereira, M.C. TGF-β receptor type II costameric localization in cardiomyocytes and host cell TGF-β response is disrupted by Trypanosoma cruzi infection. *Parasitology* **2016**, *143*.
48. Pereira, M.C. de S.; Singer, R.; Meirelles, M.N.L. Ultrastructural Distribution of Poly (A)+ RNA During Trypanosoma cruzi-Cardiomyocyte Interaction in vitro: A Quantitative Analysis of the Total mRNA Content by in situ Hybridization. *J. Eukaryot. Microbiol.* **2000**, *47*, 264–270.
49. Machado, F.S.; Martins, G. a; Aliberti, J.C.; Mestriner, F.L.; Cunha, F.Q.; Silva, J.S. Trypanosoma cruzi-infected cardiomyocytes produce chemokines and cytokines that trigger potent nitric oxide-dependent trypanocidal activity. *Circulation* **2000**, *102*, 3003–8.
50. Sun, M.; Chen, M.; Dawood, F.; Zurawska, U.; Li, J.Y.; Parker, T.; Kassiri, Z.; Kirshenbaum, L. a; Arnold, M.; Khokha, R.; et al. Tumor necrosis factor-alpha mediates cardiac remodeling and ventricular dysfunction after pressure overload state. *Circulation* **2007**, *115*, 1398–407.
51. Cuenda, A.; Rousseau, S. p38 MAP-kinases pathway regulation, function and role in human diseases. *Biochim. Biophys. Acta* **2007**, *1773*, 1358–75.
52. Stempin, C.C.; Garrido, V. V; Dulgerian, L.R.; Cerbán, F.M. Cruzipain and SP600125 induce p38 activation, alter NO/arginase balance and favor the survival of Trypanosoma cruzi in macrophages. *Acta Trop.* **2008**, *106*, 119–27.
53. Molkentin, J.D.; Bugg, D.; Ghearing, N.; Dorn, L.E.; Kim, P.; Sargent, M.A.; Gunaje, J.; Otsu, K.; Davis, J. Fibroblast-specific genetic manipulation of p38 MAPK in vivo reveals its central regulatory role in fibrosis. *Circulation* **2017**, *136*, 549–561.
54. Engel, M.E.; McDonnell, M.A.; Law, B.K.; Moses, H.L. Interdependent smad and jnk signaling in transforming growth factor- beta-mediated transcription. *J. Biol. Chem.* **1999**, *274*, 37413–37420.
55. Zhang, Y.E. Non-Smad pathways in TGF-β signaling. *Cell Res.* **2010**, *19*, 128–139.
56. Suman, S.; Rachakonda, G.; Mandape, S.N.; Sakhare, S.S.; Villalta, F.; Pratapid, S.; Lima, M.F.; Ndeid, P.N. Phospho-proteomic analysis of primary human colon epithelial cells during the early Trypanosoma cruzi infection phase. **2018**.
57. Udoko, A.N.; Johnson, C.A.; Dykan, A.; Rachakonda, G.; Villalta, F.; Mandape, S.N.; Lima, M.F.; Pratap, S.; Nde, P.N. Early Regulation of Profibrotic Genes in Primary Human Cardiac Myocytes by Trypanosoma

cruzi. *PLoS Negl. Trop. Dis.* **2016**, *10*, 1–23.

58. Wyler, D.J.; Libby, P.; Prakash, S.; Prioli, R.P.; Pereira, M.E. Elaboration by mammalian mesenchymal cells infected with Trypanosoma cruzi of a fibroblast-stimulating factor that may contribute to chagasic cardiomyopathy. *Infect. Immun.* **1987**, *55*, 3188–91.
59. Arias, J.I.; Sepulveda, C.; Bravo, P.; Hamilton-West, C.; Maldonado, I.; Ferreira, A. Comparative effect of human and Trypanosoma cruzi calreticulin in wound healing. *J. Tissue Eng. Regen. Med.* **2015**, *9*, 41–54.
60. Reis, M.M.; Higuchi, M. de L.; Benvenuti, L.A.; Aiello, V.D.; Gutierrez, P.S.; Bellotti, G.; Pileggi, F. An in situ quantitative immunohistochemical study of cytokines and IL-2R+ in chronic human chagasic myocarditis: correlation with the presence of myocardial Trypanosoma cruzi antigens. *Clin. Immunol. Immunopathol.* **1997**, *83*, 165–72.
61. Li Q, Chang L, Su DM, M.X. Effects of tetrandrine on proliferation and activation of cardiac fibroblasts. *Beijing Da Xue Xue Bao Yi Xue Ban* **2018**, *50*, 331–334.
62. Meirelles, M.N.S.L.; de Araújo-Jorge, T.C.; Miranda, C.F.; de Souza, W.; Barbosa, H.S. Interaction of Trypanosoma cruzi with heart muscle cells: ultrastructural and cytochemical analysis of endocytic vacuole formation and effect upon myogenesis in vitro. *Eur. J. Cell Biol.* **1986**, *41*, 198–206.